JTTEE5 11:218-225
© ASM International

Peer Reviewed

Microstructure and Properties of Thermally Sprayed Silicon Nitride-Based Coatings

S. Thiele, R.B. Heimann, L.-M. Berger, M. Herrmann, M. Nebelung, T. Schnick, B. Wielage, and P. Vuoristo

(Submitted 3 December 2000; revised 2 February 2001)

The preparation of thermally sprayed, dense, Si_3N_4-based coatings can be accomplished using composite spray powders with Si_3N_4 embedded in a complex oxide binder matrix. Powders with excellent processability were developed and produced by agglomeration (spray drying) and sintering. Optimization of the heat transfer into the powder particles was found to be the most decisive factor necessary for the production of dense and well-adhering coatings. In the present work, different thermal spray processes such as detonation gun spraying (DGS), atmospheric plasma spraying (APS) with axial powder injection, and high-velocity oxyfuel spraying (HVOF) were used. The coatings were characterized using optical and scanning electron microscopy (SEM), x-ray diffraction (XRD), and microhardness testing. The wear resistance was tested using a rubber wheel abrasion wear test (ASTM G65). In addition, thermoshock and corrosion resistances were determined. The microstructure and the performance of the best coatings were found to be sufficient, suggesting the technical applicability of this new type of coating.

Keywords detonation gun spraying, feedstock, microstructure, silicon nitride, wear resistance

1. Introduction

The synergy of excellent mechanical, thermal, and chemical properties of silicon nitride has made this material very attractive for structural ceramics applications.[1] However, thermal spraying of Si_3N_4 has been considered to be impossible for many years because Si_3N_4 sublimates and oxidizes at the high temperatures used in all thermal spray processes. Previous attempts to produce thermally sprayed, silicon nitride-based coatings included the use of metallic binders[2-4] as well as in situ nitridation in flight[5] or in the as-deposited state through a reactive spray process.[6] However, the anticipated high contents of Si_3N_4 in the coatings could not be realized because of either formation of embrittling silicides through reaction with the metallic binder[2-4] or very low nitridation rates.[5,6]

The most successful attempt to prepare Si_3N_4-based coatings thus far was made by Sodeoka et al.[7] using spray powders obtained from β′-SiAlON ($Si_{6-z}Al_zO_zN_{8-z}$) with different degrees of substitution, z. The powders were prepared by reacting corresponding amounts of α-Si_3N_4, Al_2O_3, and AlN at 1600 °C in a nitrogen atmosphere, crushing the product to a particle size <32 μm, and spray drying an aqueous slurry of this powder to obtain sprayable spherical granules. The 25-45 μm fraction of this spherical spray powder, consisting of β′-SiAlON and a small amount of residual alumina, was used to deposit coatings by atmospheric plasma spraying (APS) with Ar/H_2 or $Ar/H_2/N_2$ as plasma gases, with the maximum degree of substitution ($z = 4$) in all cases, and with $z = 3$ at higher plasma power. No coatings could be obtained from powders with low degrees of substitution (z = 1-2). The density (and the hardness) of the coatings increased with increasing plasma power to a maximum value of 62.5% of the theoretical density, when Ar/H_2 as plasma gases were used. The addition of nitrogen gas to the plasma gas suppressed the decomposition of the β′-SiAlON. Nevertheless, the density of the coatings with $z = 4$ was only increased to approximately 70% of the theoretical value.

Japanese patent 63-169371[8] was granted for the application of oxide-bonded SiC or Si_3N_4 coatings on Al-alloy pistons in an internal combustion engine. The (clad-type) spray powders used consisted of large SiC or Si_3N_4 grains with smaller oxide grains at their surfaces. When NiAl or NiCr bond coats were used, the top coats were claimed to have excellent hardness, adhesion strength, and resistance to heat and wear.

Because silicon nitride does not melt, but decomposes at temperatures exceeding 1900 °C, it is necessary to use composite powders similar to WC-Co, in which one component melts and simultaneously protects the other from decomposition. However, metals such as nickel[2-4] or cobalt[4] are not suitable because they form embrittling silicides. To avoid this problem, spray powders using metallic silicon or complex oxide binders were developed.[9] Preliminary experiments[10] showed that optimization of the heat transfer into the powder particles is required in order to obtain dense and well-adhering coatings. When a silicon binder and high Si_3N_4 contents were used, poor coating properties were obtained, leading to the cancellation of the powder development with this type of binder. For the oxide-bonded powders, significant progress in coating quality was made using detonation gun spray-

S. Thiele, L.-M. Berger, M. Herrmann, and **M. Nebelung,** Fraunhofer Institute of Ceramic Technology and Sintered Materials, Winterbergstrasse 28, D-01277 Dresden, Germany; **R.B. Heimann,** Freiberg University of Mining and Technology, Brennhausgasse 14, D-09596 Freiberg, Germany; **T. Schnick** and **B. Wielage,** Chemnitz University of Technology, Erfenschlager Strasse 73, D-09125 Chemnitz, Germany; and **P. Vuoristo,** Tampere University of Technology, P.O. Box 589, FIN-33101 Tampere, Finland. Present addresses: L.-M. Berger, Fraunhofer Institute of Material and Beam Technology, Winterbergstrasse 28, D-01277 Dresden, Germany; T. Schnick, GTV mbH, P.O. Box 311, D-57503 Betzdorf, Germany. Contact e-mail: thiele@ikts.fhg.de.

Table 1 Spray Powder Characteristics

Powder	Binder-Forming Additive, mass%	z in $Si_{6-z}Al_zO_zN_{8-z}$	Density, g/cm^3	a_s (BET) (m^2/g) 45-63 μm	32-45 μm	20-32 μm	Open Porosity, %
1	16 Al_2O_3, 16 Y_2O_3, 4.2 A1N, 4 SiO_2	1.7	3.30	0.21	0.28	0.34	4
2	16 Al_2O_3, 16 Y_2O_3, 4.2 A1N, 3 MgO	1.5	3.37	1.30	1.11	1.57	19
3	16 Al_2O_3, 16 Y_2O_3	3.0	3.41	1.90	…	…	29

ing (DGS) and APS (axial powder injection). Coating porosity and abrasion wear resistance were found to be dependent on the particle size distribution of the spray powder.[11] Further progress was obtained with modified powder compositions.[12]

This paper focuses on the description of the microstructure and properties of oxide-bonded Si_3N_4-based coatings obtained from three selected composite powders. Spraying was performed using DGS (Perun P, Paton Institute, Ukraine), high-velocity oxyfuel (HVOF) (Top Gun [G] GTV mbH, Luckenbach, Germany), and APS (AXIAL III, Northwest Mettech Corp., Richmond, BC, Canada) equipment.

2. Spray Powders

2.1 Spray Powder Preparation

Oxides such as Al_2O_3 and Y_2O_3 are the most commonly used sintering aids for the preparation of monolithic Si_3N_4 ceramics. The development of Si_3N_4-based powders with an oxide binder matrix is based on these fundamentals. Thus, many of the physical and chemical interactions occurring between the components are already well known. In particular, the same chemical reactions and phase transformations take place during sintering of the spray powder as during sintering of conventional Si_3N_4 ceramics. However, it is known that the thermal spray process requires a minimum amount of a meltable binder for good sprayability of composite powders. In commercially available carbide-metal binder composite powders, such as WC-Co, the binder content is 20-30 vol.%.[13] Therefore, compared with conventional ceramics, oxide-bonded Si_3N_4-based spray powders have an increased oxide content. After the characteristic phases and microstructure are formed in the sintering step of the powder preparation process, the oxide binder assumes the function of the component that melts during the spray process. Simultaneously, the oxide binder phase should protect the silicon nitride from oxidation and/or evaporation during thermal spraying.

The compositions and the most important parameters of the spray powders are compiled in Table 1. All powders were prepared by mixing of the individual components by agglomeration (spray drying) and subsequent sintering. If the parameters of the spray drying process are properly selected and carefully controlled, powders with the required particle size range and of nearly ideal spherical shape will be obtained. For preparation of powders 1 and 2, finely dispersed silicon nitride powders with an α-Si_3N_4 content of >70% were used with the binder-forming additives listed in Table 1 as starting materials. The addition of SiO_2 or MgO in powders 1 and 2, respectively, decreases the viscosity of the oxide binder matrix, while the addition of AlN promotes the formation of SiAlON. To prepare spray powder 3, a β'-SiAlON with $z = 3$ was used instead of silicon nitride powder. This finely dispersed starting powder was obtained by reacting a mixture of Si_3N_4, Al_2O_3, and AlN powders and subsequently milling the resultant powder. After the organic binder of the spray-dried granules was removed by heating, the spray powders were sintered in a nitrogen-containing atmosphere, subsequently mechanically treated by a mild milling process, and finally fractionized by sieving. For the fundamental investigations of this work, fractions narrower than those normally known for commercial spray powders were used (20-32, 32-45, and 45-63 μm).

2.2 Spray Powder Characterization Methods

The morphology of ceramographically prepared cross sections of the powders was investigated by scanning electron microscopy (SEM). The porosity of the spray powders was determined by measuring the nitrogen adsorption isotherms and the mercury intrusion with an ASAP 2010 and a Poresizer 9320, respectively (both by Micromeritics, Norcross, GA). From the nitrogen adsorption isotherms, the specific surface areas, a_s, according to Brunauer-Emmett-Teller (BET) and the pore size distributions were calculated. The mercury intrusion plots were obtained using the equilibrium measurement mode (equilibrium time of 20 s). The densities of the powders were measured by a helium pycnometer (Accupyc 1305, Micromeritics). Phase compositions were determined by x-ray diffraction (XRD) using Co-Kα radiation (XRD7, Seifert, Germany). The average z values were obtained by Rietveld refinement. Oxygen and nitrogen contents were measured using a model TC-436 analyzer (LECO Corporation, St. Joseph, MO).

2.3 Spray Powder Properties

The typical morphology of the spray powder particles is shown in Fig. 1. The granules of all powders used in this work have a nearly spherical shape. The micrographs of the cross sections of powders 1-3 are shown in Fig. 2(a-c), respectively. Powder 1 is made up of fully dense particles, whereas powder 2 is made up of coexisting porous and dense particles. Powder 3 is porous, but larger pores are absent. The densities measured by helium pycnometry (Table 1) correspond with the theoretical densities. Thus, virtually no closed porosity exists in the spray powders.

The pore size distributions calculated from the nitrogen adsorption isotherms showed no open pores (pore sizes detectable by this method range from 0.4 to approximately 250 nm). This is in agreement with the results of mercury porosimetry for pore sizes of <250 nm. The values of the specific surface areas are

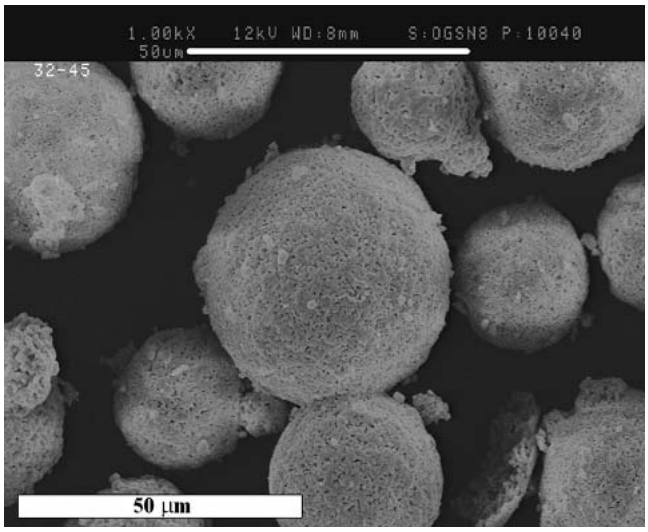

Fig. 1 Typical morphology of powder particles

compiled in Table 1. As expected, the specific surface area of the dense powder 1 increases with decreasing particle size. The higher specific surface areas of powders 2 and 3 result from the inner porosity existing in the powders. However, the distribution of the porosity in powder 2 seems to be inhomogeneous in the fractions investigated, because no dependence on the powder particle size could be detected.

Figure 3 shows plots of pore size distributions obtained by mercury intrusion into the fractions 45-63 µm for powders 1 to 3. With the available equipment, open pores in the size range 6 nm-200 µm can be investigated. However, interpretation of the pore size distributions of spray powders is complicated by the fact that at the filling pressure, mercury intrusion into the voids between the individual spray powder particles is not yet complete. Because the intrusion pressure depends on the particle size, the measurements were performed for the largest fractions, for which this effect can best be distinguished from the existing porosity. The peaks with a maximum somewhat higher than 10 µm that appear in all powders are caused by this intrusion into the voids between the spray powder particles. A partial overlap of this effect with the effect of intrusion into much smaller intraparticle pores cannot been excluded. Hence, the open porosities of the powders were calculated using the results from mercury intrusion into pores <5 µm, as given in Table 1.

The spray powders consist of β′-SiAlONs embedded in an amorphous binder matrix. During sintering of the spray powder, partial transformation of metastable α-Si_3N_4 to β-Si_3N_4 takes place by solution and reprecipitation processes. The complete reaction in the temperature range 1450-1900 °C can be described schematically as follows:

$$Si_3N_4 + Al_2O_3 + Y_2O_3 + SiO_2 \rightarrow Si_{6-z}Al_zO_zN_{8-z} + \text{Y-Si-Al-O-N-glass} \quad \text{(Eq 1)}$$

The high oxide content (compared with that of conventional Si_3N_4 ceramics) and the relatively slow cooling rate below 1450 °C lead to the formation of the crystalline oxide phase $Y_3Al_5O_{12}$

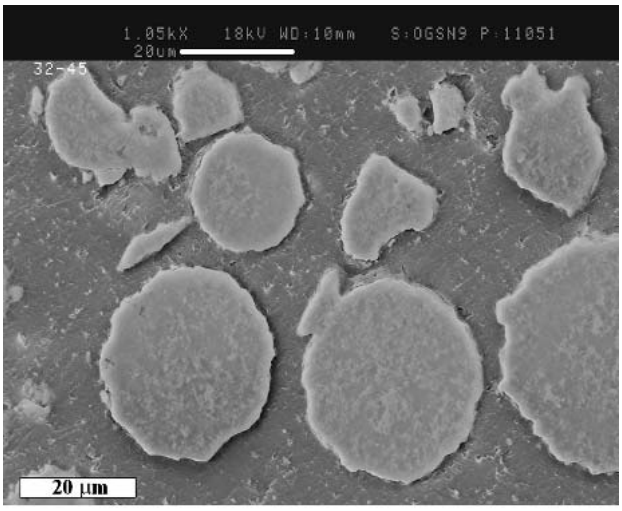

(a)

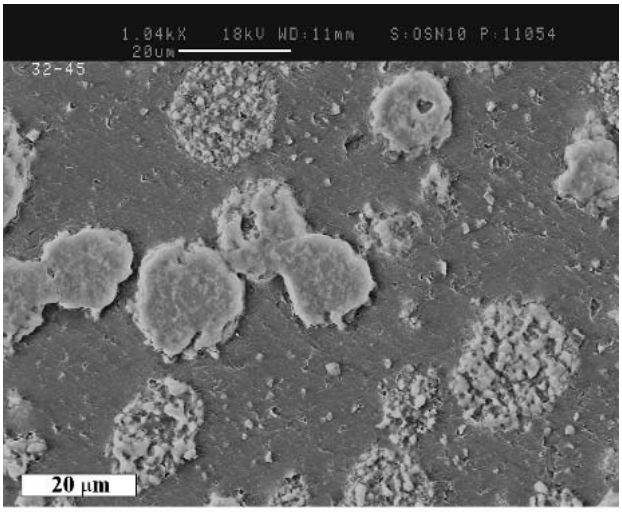

(b)

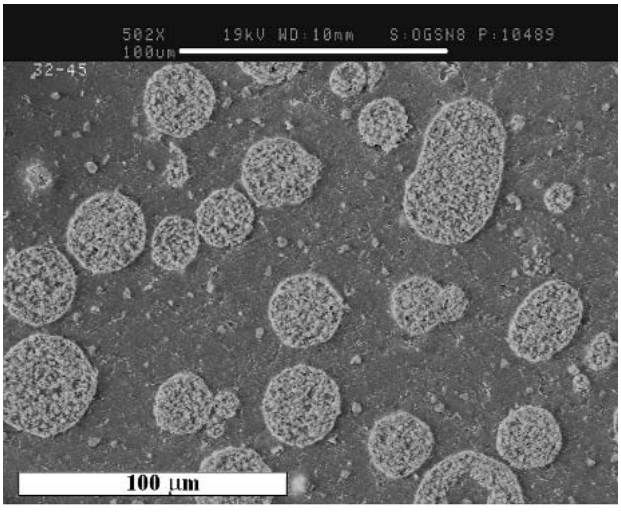

(c)

Fig. 2 **(a)** Cross section of spray powder 1; **(b)** cross section of spray powder 2; **(c)** cross section of spray powder 3

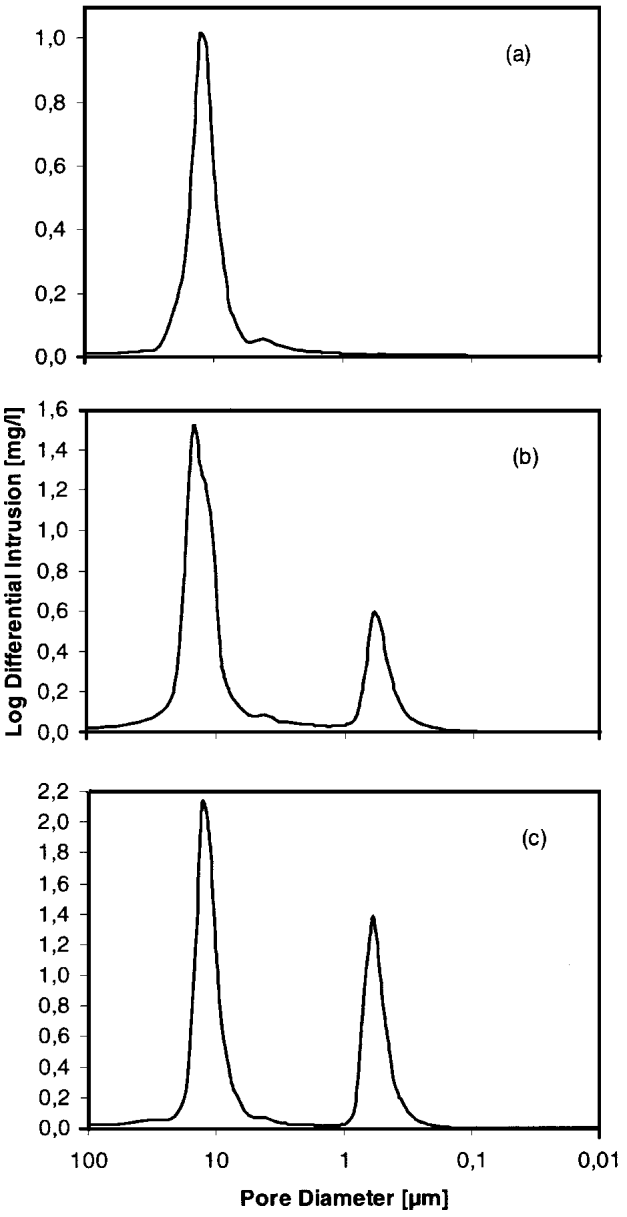

Fig. 3 Pore size distribution plots obtained by mercury porosimetry **(a)** powder 1, **(b)** powder 2, **(c)** powder 3

(YAG) in the spray powder preparation process (Fig. 4). Simultaneously, formation of β′-SiAlONs ($Si_{6-z}Al_zO_zN_{8-z}$) takes place as a result of the substitution of Si and N by Al and O, respectively. The transformation of Si_3N_4 into SiAlON is incomplete due to the low sintering temperatures. The average values of *z*, characterizing the degree of substitution in the crystal lattice, are also given in Table 1. In powder 3, prepared using SiAlON powder as a starting component, further substitution reactions do not take place on a practical scale during sintering of the spray powder. Therefore, spray powder 3 differs from powders prepared by Sodeoka et al.[7] in that it contains a binder phase in addition to β′-SiAlON. The oxygen and the nitrogen contents of powders 1 and 3 are listed in Table 2.

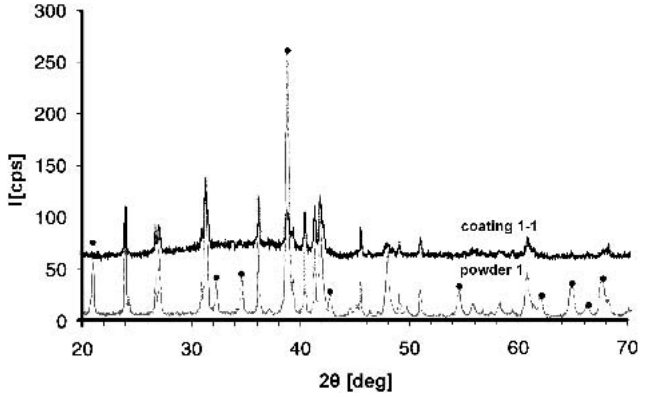

Fig. 4 Comparison of x-ray diffraction patterns for spray powder and coating (powder 1). Marked peaks relate to YAG.

Table 2 Oxygen and Nitrogen Contents of Spray Powders and Coatings

Sample	O_2-mass%	N_2-mass%
Powder 1	13.2	26.0
Coating	21.2	17.4
Powder 3	21.7	17.5
Coating	27.6	10.8

3. Spray Processes

3.1 Spray Parameters

DGS experiments were carried out at Tampere University of Technology with a Perun P gun, having a barrel 660 mm in length and 21 mm in diameter. The average firing rate was 6.6 shots/s and the spray distance was 150 mm. Thirty passes were sprayed to obtain one coating of about 150 µm in thickness. The explosive gas used consisted of a mixture of acetylene and oxygen. The oxygen-to-fuel ratio was adjusted for maximum heat transfer to the spray particles in the range 1.3 to 2.3. The acetylene gas flow rate was kept constant at 11 SLPM. The oxygen-to-fuel ratio of 1.3 corresponded to a flow rate of 14 SLPM oxygen; the ratio of 2.3 to a flow rate of 25 SLPM oxygen. No diluent gas was used. Low carbon steel was used as a standard substrate. Powders 1 and 2 (both with a particle size of 20-32 µm) were also deposited onto Inconel600 substrates for the evaluation of their thermoshock resistance. For these investigations, a NiCrAlY bond coat was applied by APS spraying.

HVOF spray experiments were performed with a Top Gun (gas) system. A large combustion chamber (length of 22 mm) in combination with a 200 mm nozzle was used. The fuel gas used was ethylene. The oxygen-to-fuel ratio was varied between 1.5 and 3.3. The spray distance ranged from 200-250 mm. The experiments were carried out only with spray powder 2.

The APS experiments were performed using an AXIAL III plasma spray system. The operating principle differs from that of conventional plasma spray equipment by the axial powder injection mode and thus the plasmatron configuration. In this construction, three anodes and cathodes are located symmetrically around the powder injection tube. The very high plasma power and the axial powder injection that places the powder par-

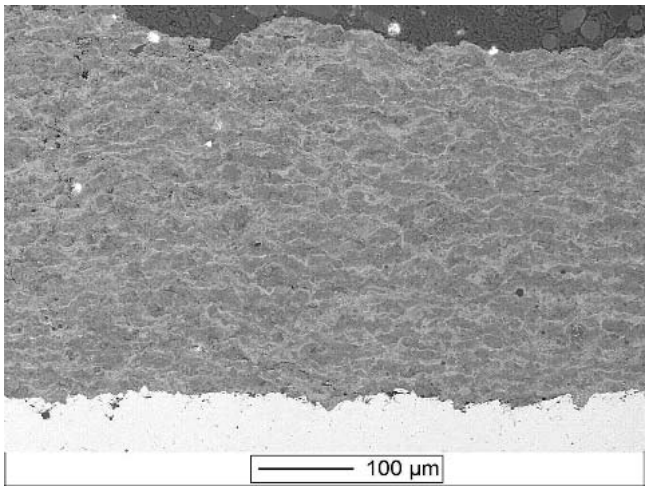

Fig. 5 SEM micrograph of a D-Gun-sprayed coating (powder 2, 20-32 µm)

ticles in the center of the plasma jet result in better heat transfer into the powder particles than that obtained using conventional plasmatrons. The experiments were performed using spray powder 3 and a mixture of N_2/H_2 (ratio of 2.6) as the plasma gas. The plasma power was 115 kW; the spray distance was 140 mm.

3.2. Coating Characterization

The microstructures of the coatings were studied by optical microscopy and SEM. The amount of porosity was determined by image analysis. Phase compositions of all coatings were investigated by XRD in the same manner as for the spray powders. Oxygen and nitrogen contents of powderized coatings were determined. Hardness testing was performed using a Vickers microhardness tester, with an indentation load of 50 g and 10 measurements for each sample. The abrasion wear resistance was determined according to ASTM G 65 using a rubber wheel abrasion wear test apparatus (load of 13 N, wear path length of 5904 m, quartz sand grain size of 0.1-0.6 mm). The thermal shock resistance was investigated by heating the coated substrates in a furnace up to 800 °C and subsequently quenching to about 150 °C in air (cooling rate of about 8 K/s). Experiments with rapid cooling to room temperature were carried out by dropping the sample into a container filled with water. The thermoshock resistance was investigated for coatings of powders 1 and 2 on Inconel600 substrates with NiCrAlY bond coats. The corrosion resistances of the coatings were investigated using a salt spray test according to ASTM B 117-73 (DIN 50021). A NaCl solution was sprayed onto the surfaces of the coatings (substrates were masked with a resin) at a temperature of 35 °C for 23 h. The amount of corrosion products on the coating surface was estimated for each sample using optical image analysis.

Characterization of the HVOF and APS coatings was limited to optical microscopy, XRD studies (APS coatings), and determination of the abrasion wear resistance (HVOF coatings).

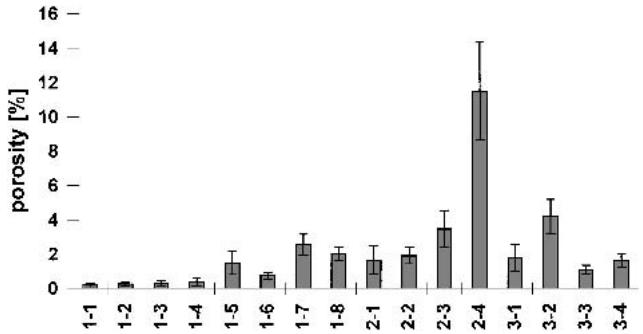

Fig. 6 Porosity of the D-Gun-sprayed coatings

Table 3 Parameters for D-Gun-Sprayed Samples

Sample	Powder	Particle Size, µm	Oxygen-to-Fuel Ratio
1-1	1	20 to 32	1.9
1-2	1	20 to 32	1.2
1-3	1	20 to 32	1.5
1-4	1	20 to 32	2.2
1-9	1	20 to 32	1.9
2-1	2	20 to 32	1.9
2-2	2	20 to 32	1.2
2-5	2	20 to 32	1.9
3-1	3	20 to 32	1.9
3-2	3	20 to 32	1.2
3-5	3	20 to 32	1.9
1-5	1	32 to 45	1.9
1-6	1	32 to 45	2.2
2-3	2	32 to 45	1.9
3-3	3	32 to 45	1.2
3-4	3	32 to 45	1.9
3-6	3	32 to 45	1.9
1-7	1	45 to 63	1.9
1-8	1	45 to 63	2.2
2-4	2	45 to 63	1.9
3-7	3	45 to 63	1.9

4. Results and Discussion

4.1 DGS Coatings

4.1.1 Coating Structures. For all spray powders listed in Table 1, well-adhering coatings were obtained by detonation gun (D-Gun) spraying onto mild steel substrates without a bond coat.

Figure 5 shows an SEM micrograph of a coating produced from powder 2 (20-32 µm). The coating has a homogeneous microstructure and is nearly completely dense. In earlier experiments,[11,12] it was found that the microstructure of the coatings primarily depends on the properties of the spray powders, in particular the particle size; i.e., the larger the particle size, the higher the porosity and the heterogeneity of the coating, results that are thought to be caused by insufficient melting of the larger particles.

As shown in Fig. 6, the porosities of the D-Gun-sprayed coatings are generally very low. The sample numbers, the corresponding particle size fractions, and the oxygen-to-fuel ratios

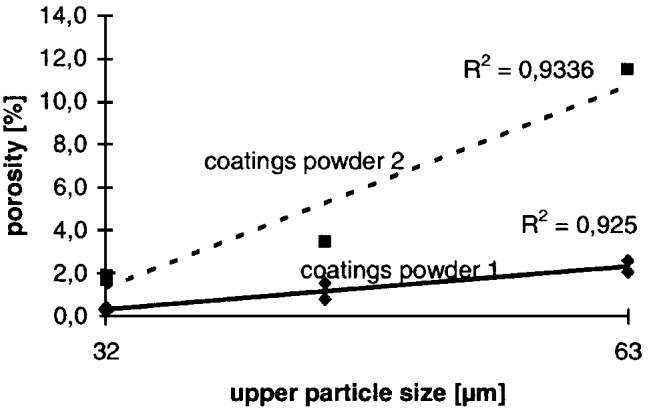

Fig. 7 Correlation between particle size and porosity of D-Gun sprayed coatings

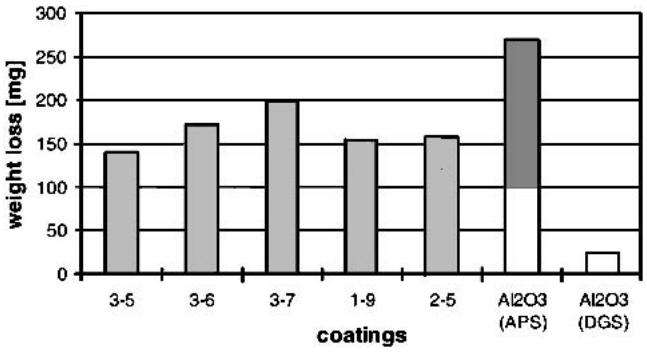

Fig. 8 Comparison of the abrasion wear resistance of D-Gun-sprayed Si_3N_4-based coatings and DGS and APS Al_2O_3-coatings (3-5, 1-9, 2-5: 20 to 32 µm; 3-6: 32 to 45 µm; 3-7: 45 to 63 µm)

are given in Table 3. The lowest porosities were obtained for powder 1. Coatings produced from the largest fraction (45-63 µm) still exhibit porosities <3%, in the case of powder 2 for this fraction (sample 2-4) the porosities were exceptionally large. As shown in Fig. 7, coatings obtained from powders 1 and 2 show a statistically highly significant linear relation between porosity and spray powder particle size. The correlation coefficients, *R*, correspond to 0.96 and 0.97 for powders 1 and 2, respectively. The larger the particle size, the less effective the heating, and the larger the voids formed in the coatings because of incomplete filling by the consecutively arriving spray particles.

The differences in the XRD patterns of the coatings obtained under various spray conditions were small, demonstrating the high stability of the phases in these spray powders. The XRD patterns of powder 1 and coating 1-1 are shown in Fig. 4; α- and β-Si_3N_4 are the dominating phases in this and the other coatings. There is no further phase transformation from α-Si_3N_4 to β-Si_3N_4 in the D-Gun-sprayed coatings after initial spraying, presumably due to the low process temperature and the short dwell time. As expected, YAG significantly decreased in amount, almost disappearing (Fig. 4). This phase melts during the spray process and dissolves in the amorphous binder phase. Comparison of the oxygen and nitrogen contents of the spray powders and coatings given in Table 2 shows that the amount of oxygen increases by about 7 mass% and the nitrogen content decreases simultaneously by about 7 mass% during spraying. From these values, a decrease in the overall silicon nitride content of about 25 mass% can be estimated. This portion was oxidized during spraying and formed a glassy phase with the sintering aids, the amount of which can be estimated to be approximately 50%.

4.1.2 Coating Properties. The microhardness of the D-Gun coatings sprayed with different conditions was found to lie in the range 379-472 $HV_{0.05}$ (powder 1), 411-638 $HV_{0.05}$ (powder 2), and 471-563 $HV_{0.05}$ (powder 3). These rather low values cannot be explained by the existence of high porosity in the coatings. Hence, this fact clearly demonstrates that the determination of the indentation microhardness of thermally sprayed coatings and the interpretation of the results may be problematic because of the generally heterogeneous microstructure of such coatings and the presence of a relatively high amount of glassy phase. Consequently, estimation of the wear resistance of the coatings probably gives a much more pertinent reflection of their technological performance.

The abrasion wear tests revealed that coatings produced from coarse powders with a particle size of 45-63 µm showed a noticeably worsened wear performance. However, below this threshold, the differences in the wear performances of the coatings were relatively small. Selected coatings were tested and compared with plasma-sprayed alumina coatings (Fig. 8). The decrease in abrasion wear resistance with increasing spray powder particle size was demonstrated for powder 3. The results for the 20-32 µm fraction were approximately identical for all three powders. All D-Gun-sprayed coatings were found to be comparable to plasma-sprayed alumina coatings. The large spread in the wear performance of the plasma-sprayed alumina coatings represented by the dark bar reflects the influence of the state of the electrode pairs, representing different lifetimes.

The thermal shock resistance of the coatings depends not only on porosity and Young's modulus, but also on differences in the coefficients of thermal expansion between the substrate and the coating material.[14] Hence, for the preparation of a highly thermoshock-resistant system, Inconel600 substrates coated with NiCrAlY bond coats were used. Furthermore, the coating thickness was adjusted to 70-100 µm. Coatings sprayed with powders 1 and 2 were tested 10 times using air cooling and six times using water cooling. The coatings showed small spallations at the edges, but no further damage (Fig. 9). The absence of a bond coat caused immediate spalling of the whole coating, indicating that the stress at the interface between coating and substrate was too large to be able to relax without damaging the composite. However, the low number of test cycles and the simple preliminary test procedure allowed only a tentative estimation of the thermal shock resistance to be made at this point. In the salt spray corrosion tests of samples with sufficiently thick and homogeneous coatings, the amount of corrosion products on the surface was found to be about 2% (ratio of amount of corroded surface to whole surface).

4.2 Top Gun and APS coatings

Figure 10 shows the microstructure of a Top-Gun-sprayed sample (powder 2, 32-45 µm fraction). In comparison to the D-Gun-sprayed coatings, these coatings show highly heteroge-

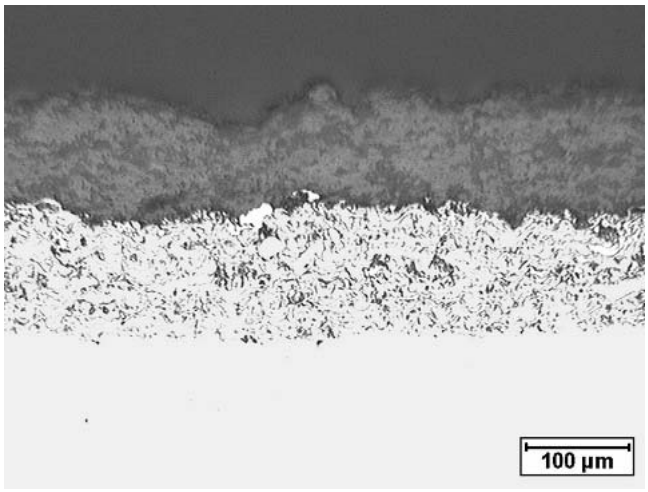

Fig. 9 Optical micrograph of a D-Gun-sprayed coating (powder 1, 32 to 45 µm) with a bond coat after thermal shock resistance testing

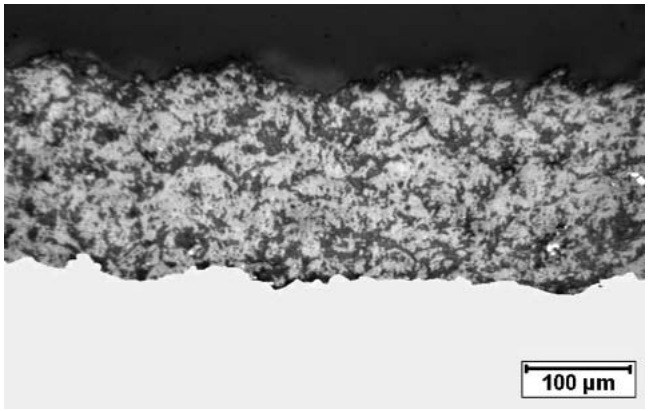

Fig. 10 Optical micrograph of a Top-Gun-sprayed coating (powder 2, 32 to 45 µm)

neous microstructures (Fig. 5). The best results were obtained using an oxygen-to-fuel ratio of 1.5. Results of the rubber wheel test (ASTM G65) showed that the best coating has a wear resistance comparable to that of the D-Gun-sprayed coatings.

Figure 11 shows an optical micrograph of the cross section of an APS-sprayed coating with an optimized microstructure (powder 3, 45-63 µm fraction), composed of areas of high density interspersed with highly porous regions. This porosity should be able to be reduced by further process optimization as well as by the use of smaller particle size fractions. XRD analysis showed β′-SiAlON as the dominant crystalline phase.

5. Conclusions

Dense Si_3N_4-based coatings were produced using oxide-bonded Si_3N_4 composite powders and different thermal spraying techniques. This represents significant progress in the thermal spraying of silicon nitride, which up to now has been considered a nonsprayable material. Spray powders of different

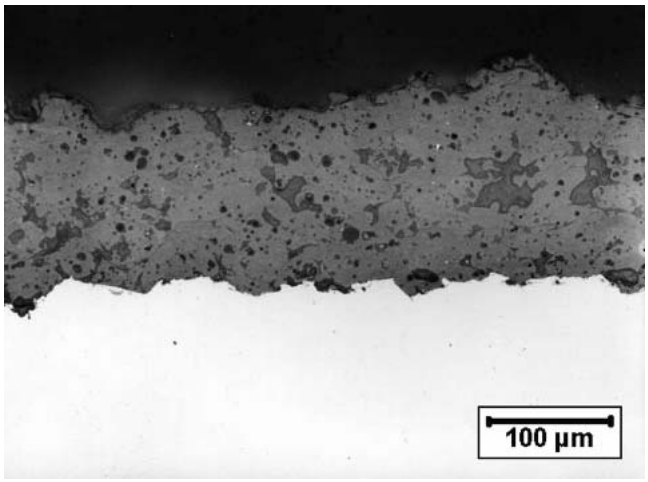

Fig. 11 Optical micrograph of an APS-sprayed coating (powder 3, 45 to 63 µm)

oxide binder matrix composition and porosity were investigated. The interactions between these parameters as well as the choice of the thermal spray technique were evaluated. The spray powder particle size appears to be the most important factor up to a certain threshold. A clear picture of the role of the chemical composition was not obtained for the powders investigated in this work.

In D-Gun spraying, the oxygen-to-fuel ratio is an important process parameter. Optimization of the heat transfer into the powder particles was found to be the most decisive factor necessary for the production of dense and well-adhering coatings.

The best coatings showed a wear resistance comparable to that of conventional plasma-sprayed alumina coatings, when subjected to a rubber wheel abrasion wear test (ASTM G65). Such dense Si_3N_4-based coatings on steel and Inconel substrates also exhibited satisfactory corrosion and thermoshock resistances in preliminary tests. On the basis of these experimental results, it appears to be possible to suggest the technical application of this new type of coating.

Acknowledgments

Support of this research by the Deutsche Forschungsgemeinschaft (German Science Foundation) under the grants He 923/4-2, Wi 688/15-2, and He 2457/1-2 is gratefully acknowledged. The authors are indebted to Euromat GmbH, Hückelhoven, Germany, for performing the spray experiments with the Mettech AXIAL III gun, and to Dr. K. Nassenstein, GTV mbH, Luckenbach, Germany, for providing the Top Gun spray experiments. The oxygen and nitrogen analyses were performed by Dr. W. Gruner (IFW Dresden, Germany).

References

1. L. Michalowsky, ed.: *New Ceramic Materials*, Deutscher Verlag für Grundstoffindustrie, Leipzig, Stuttgart, 1994 (in German).
2. E. Lugscheider and R. Limbach: *Plasma Spraying of Agglomerated Powders on the Basis of Si_3N_4*, DVS Berichte, 130, Deutscher Verlag für Schweisstechnik, Düsseldorf, 1990, pp. 224-25 (in German).
3. E. Lugscheider, R. Limbach, A. Liden, and J. Lodin: "Plasma Spraying

of Silicon Nitride (Si_3N_4)" in *Proc. Conf. High Temp. Mater. Powder Eng.,* Liege, Belgium, *1,* F. Bachelet, ed., Kluwer, Dordrecht, The Netherlands, 1990, pp. 877-80.

4. R. Limbach: "Development of Thermally Sprayed Wear Resistant Coatings with Favorable Tribological Behavior," Techn.-Wiss. Berichte Lehr- und Forschungsgebiet Werkstoffwissenschaften der RWTH Aachen Nr. 37.03.12.92, E. Lugscheider, ed., 1992 (in German).
5. T. Eckardt, W. Malléner, and D. Stöver: "Reactive Plasma Spraying of Silicon in Controlled Nitrogen Atmosphere" in *Thermal Spray Industrial Applications*, C.C. Berndt and S. Sampath, ed., ASM International, Materials Park, OH, 1994, pp. 515-19.
6. T. Eckardt, W. Malléner, and D. Stöver: "Development of Plasma Sprayed Silicon/Silicon Nitride Coatings by In-Situ Nitridation" in *Thermische Spritzkonferenz: TS96*, E. Lugscheider, ed., DVS Berichte, 175, Dt. Verl. für Schweisstechnik, Düsseldorf, 1996, pp. 309-12 (in German).
7. S. Sodeoka, K. Ueno, Y. Hagiwara, and S. Kose: "Structure and Properties of Plasma-Sprayed Sialon Coatings," *J. Thermal Spray Technol.*, 1992, *1*, pp. 153-59.
8. T. Tomota, N. Miyamoto, and H. Koyama: Formation of Thermal Spraying Ceramic Layer, Patent JP 63 169371, A, Int. Cl.[4]: C23C 4/10, Filing date 29.12.1986, Publication date 13.07.1988, Patent Abstracts of Japan, 12, No. 446, 24.11.1988 (in Japanese).
9. L.-M. Berger, M. Herrmann, M. Nebelung, R.B. Heimann, and B. Wielage: Modified Composite Silicon Nitride Powders for Thermal Coating Technologies and Process for Their Production, German Patent DE 196 12 926, C2, Int. Cl.[6]: C04B 35/587, C23C 4/10, Filing date 01.04.1996, Publication date 30.09.1999; United States Patent US 6,110,853, Int. Cl.[7]: C04B 35/596, C04B 35/599, Filing date 11.02.1999, Publication date 29.08.2000.
10. S. Thiele, R.B. Heimann, M. Herrmann, L.-M. Berger, M. Nebelung, M. Zschunke, and B. Wielage: "Thermal Spraying of Silicon Nitride-Based Powders" in *Thermal Spray: Practical Solutions for Engineering Problems*, C.C.Berndt, ed., ASM International, Materials Park, OH 1996, pp. 325-31.
11. L.-M. Berger, M. Herrmann, M. Nebelung, S. Thiele, R.B. Heimann, T. Schnick, B. Wielage, and P. Vuoristo: "Investigations on Thermal Spraying of Silicon Nitride-based Powders" in *Thermal Spray: Meeting the Challenges of the 21st Century*, C. Coddet, ed., ASM International, Materials Park, OH, 1998, pp. 1149-54.
12. R.B. Heimann, S. Thiele, L.-M. Berger, M. Herrmann, M. Nebelung, B. Wielage, T. Schnick, and P. Vuoristo: "Thermally Sprayed Silicon Nitride-Based Coatings on Steel for Application in Severe Operation Environments: Preliminary Results" in *Microstructural Science: Analysis of In-Service Failures and Advances in Microstructural Characterization, 26,* E. Abramovici, D.O. Northwood, M.T. Shehata, and J. Wylie, ed., ASM International, Materials Park, OH, 1998, pp. 389-94.
13. L.-M. Berger, W. Hermel, P. Vuoristo, T. Mäntylä, W. Lengauer, and P. Ettmayer: "Structure and Properties of Hardmetal-like Coatings Prepared by Thermal Spray Processes" in *Advances in Hard Materials Production*, European Powder Metallurgy Association, Shrewsbury/U.K., 1996, pp. 443-50.
14. L. Pawlowski: *The Science and Engineering of Thermal Spray Coatings*, John Wiley & Sons, Chichester, U.K., 1995.